LUND UNIVERSITY

Bandwidth-Constrained Capacity Bounds on MIMO Antennas

Ehrenborg, Casimir; Gustafsson, Mats; Capek, Miloslav

2019

Link to publication

Citation for published version (APA):
Ehrenborg, C., Gustafsson, M., & Capek, M. (2019). *Bandwidth-Constrained Capacity Bounds on MIMO Antennas*. (TEAT; No. 7266). Electromagnetic Theory Department of Electrical and Information Technology Lund University Sweden.

Total number of authors:
3

General rights
Unless other specific re-use rights are stated the following general rights apply:
Copyright and moral rights for the publications made accessible in the public portal are retained by the authors and/or other copyright owners and it is a condition of accessing publications that users recognise and abide by the legal requirements associated with these rights.
• Users may download and print one copy of any publication from the public portal for the purpose of private study or research.
• You may not further distribute the material or use it for any profit-making activity or commercial gain
• You may freely distribute the URL identifying the publication in the public portal

Read more about Creative commons licenses: https://creativecommons.org/licenses/

Take down policy
If you believe that this document breaches copyright please contact us providing details, and we will remove access to the work immediately and investigate your claim.

LUND UNIVERSITY

PO Box 117
221 00 Lund
+46 46-222 00 00

CODEN:LUTEDX/(TEAT-7266)/1-26/(2019)
Revision No. 1: June 2020

Bandwidth-Constrained Capacity Bounds on MIMO Antennas

Casimir Ehrenborg, Mats Gustafsson, and Miloslav Capek

Electromagnetic Theory
Department of Electrical and Information Technology
Lund University
Sweden

(TEAT-7266)/1-26/(2019): C. Ehrenborg, M. Gustafsson and M. Capek, Bandwidth-Constrained Capacity Bounds

Casimir Ehrenborg
casimir.ehrenborg@eit.lth.se

Department of Electrical and Information Technology
Electromagnetic Theory
Lund University
P.O. Box 118
SE-221 00 Lund
Sweden

Mats Gustafsson
mats.gustafsson@eit.lth.se

Department of Electrical and Information Technology
Electromagnetic Theory
Lund University
P.O. Box 118
SE-221 00 Lund
Sweden

Miloslav Capek
miloslav.capek@fel.cvut.cz

Department of Electromagnetic Field,
Faculty of Electrical Engineering,
Czech Technical University in Prague,
166 27 Prague,
Czech Republic

This is an author produced preprint version as part of a technical report series from the Electromagnetic Theory group at Lund University, Sweden. Homepage http://www.eit.lth.se/teat

Editor: Mats Gustafsson
© Casimir Ehrenborg, Mats Gustafsson and Miloslav Capek, Lund, September 10, 2019

Abstract

The optimal spectral efficiency of MIMO antennas in Rayleigh and ideal channels are investigated when bandwidth requirements are placed on the antenna. By posing the problem as a convex optimization problem restricted by the port Q-factor a semi-analytical expression is formed for its solution. The antennas are simulated by method of moments and the solution is formulated both for structures fed by discrete ports, as well as for design regions characterized by an equivalent current. It is shown that this solution is solely dependent on the so-called energy modes of the antenna. These modes are compared to the characteristic modes and how to effectively excite them is investigated for a linear dipole array as well as a plate with embedded, and raised, antenna regions. The performance is illustrated through spectral efficiency over the Q-factor, a quantity that is connected to the true capacity. It is demonstrated that the Q-factor and the spectral efficiency form a Pareto trade-off bound, and that a certain Q-factor is Pareto optimal.

1 Introduction

Modern communication systems often make use of multiple-input-multiple-output (MIMO) antennas. They utilize spatial multiplexing to dramatically increase the transmitted bit-rate, or capacity, in comparison to single antenna systems [33, 34]. The optimal performance of MIMO systems is therefore a topic of great interest. Many different methods have been developed to evaluate maximum capacity under different conditions and assumptions. For example by considering spherical regions [9, 13], or treating the problem through an information theoretical approach [8, 26, 30, 31, 37]. In [6, 7] the authors presented a novel method for calculating optimal spectral efficiency of arbitrary antenna designs using convex current optimization.

Design of MIMO antennas is based on effectively exciting discrete communication channels with low correlation [34]. A proposed strategy for accomplishing this is to design the antennas such that they effectively excite modes with orthogonal radiation patterns, such as characteristic modes [1, 27, 28, 29]. A modal analysis method for analyzing MIMO antennas design, constrained by radiation efficiency, was presented in [7]. This method is based on analyzing the eigenvalues of a set of modes known as radiation modes to predict the performance of a MIMO antenna. It was developed by observing that the eigenvalues of these modes played a major part in the solution to the optimal spectral efficiency constrained by radiation efficiency. However, one of the open questions of this technique is if it can be generalized to other constraining parameters, such as bandwidth.

Electrically small antennas suffer from a degradation in possible performance as their size is reduced compared to the wavelength. Some of the parameters where this is most evident are radiation efficiency, directivity, and bandwidth [16, 18, 41, 42]. Bandwidth can be estimated, for electrically small systems, through the Q-factor defined as the quotient of energy stored in a system over energy dissipated by it [36]. This relation accurately estimates the bandwidth, for single feed, single resonance systems [44], however, it does not hold for multi-port systems. In this paper this

is addressed by considering a multi-port system as a superposition of single port systems. Each port has a well defined Q-factor calculated from the stored energy of the current induced by that port [39]. These port currents make up the total current distribution on the antenna when added together. The Q-factor of the total current is therefore an implicit indication of the Q-factor in each port. In this way, restricting the Q-factor of the total current density implicitly imposes a bandwidth requirement on the system.

The optimal spectral efficiency in [6, 7] is calculated from current optimization. This is a method used for calculating the optimal performance of a design region by optimizing a current distribution within that region [15]. This current has the ability to express all possible solutions that could be created within the considered region. Controlling the current at every point in a region allows for the creation of current distributions that are not realizable by physical feeding mechanisms. However, these distributions still obey Maxwell's equations. Therefore, the optimal value obtained from current optimization bounds any value that can be obtained by antennas designed in the region.

Optimizing the current over an antenna can be computationally expensive due to the large number of unknowns involved in accurately meshing a structure. However, the problem can be recast in a smaller feeding region [7]. This can be extended to recasting the problem in only the port voltage excitation of an antenna structure. This allows for the calculation of a numerically efficient bound for existing antenna structures, such as arrays. Another advantage is the feasibility of this bound via direct realization of the port voltage excitation proposed by the optimization routine.

The optimization problem in [6, 7] is formulated as a convex optimization problem. Convex problems are defined as problems where all local minima are also global minima [2]. This means that a solution to a convex problem is guaranteed to be optimal. Previously, this method has been used to determine performance bounds for antennas in terms of, *e.g.*, Q-factor [15, 16, 24], efficiency [12, 25], directivity [14], and spectral efficiency [6, 7]. For single feed, single resonance antennas these problems can be solved efficiently due to being expressed as quadratic forms. However, spectral efficiency is evaluated based on the covariance of the current distribution and as such cannot be formulated as a quadratic form. The capacity expression creates a semi-definite optimization problem which has one order more of unknowns, making it computationally demanding to solve [6]. In [7] a method for solving such problems was introduced. By formulating a dual of the optimization problem [2] and utilizing the good properties of the matrices restricting it, it is possible to solve it semi-analytically.

In this paper optimal spectral efficiency is calculated using the computationally efficient method from [7] for MIMO antennas transmitting in an uniform multipath environment restricted by a required Q-factor. It is shown that the modal analysis method in [7] can be applied to MIMO antennas restricted by the Q-factor by considering a different set of modes called energy modes. This method is applied to an array of dipole antennas optimized through their port quantities, and antenna sub-regions within a larger device optimized through their currents. The antennas are optimized in a Rayleigh channel as well as without channel perturbation. It is

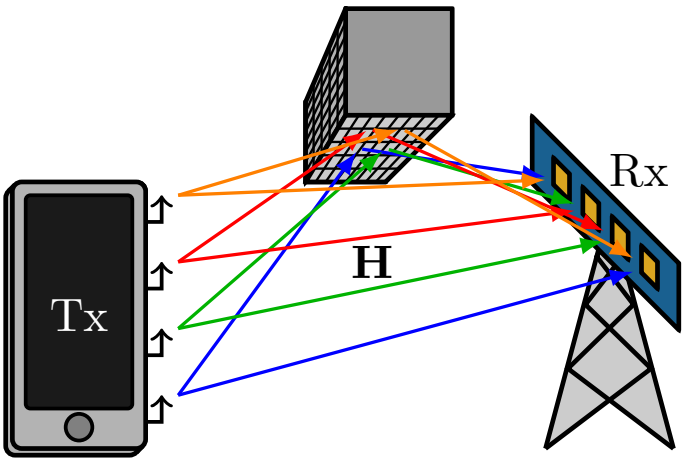

Figure 1: Schematic illustration of a MIMO system.

shown that the Rayleigh channel has only a small effect on the magnitude of the optimal spectral efficiency.

The paper is organized in the following way. In Sec. 2 the full-wave MIMO system is introduced and the effect of the channel on systems with few ports is discussed. In Sec. 3 the optimization problem is stated and solved for port quantities. The behaviour of the solution is investigated in three subsections: two dipoles are optimized at varying distance from each other in Sec. 3.2, two dipoles are investigated at different angles in Sec. 3.3, and an increasing number of dipoles in a linear array are solved in Sec. 3.4. In Sec. 4 the optimization problem is stated and solved using the current density of the antenna. The dependence on the Rayleigh channel is investigated in Sec. 4.1. In Sec. 4.2 a few antenna sub-regions are optimized while they are embedded in a device and raised above it. The paper is concluded in Sec. 5

2 Full-wave Model of MIMO Systems

A MIMO system, like the one shown in Fig. 1, is described by

$$\mathbf{y} = \mathbf{H}\mathbf{x} + \mathbf{n}, \tag{2.1}$$

where $\mathbf{y}$ is an $M \times 1$ vector containing the received signals, $\mathbf{H}$ is an $M \times N$ matrix known as the channel matrix, $\mathbf{x}$ is an $N \times 1$ vector containing the input signals, and $\mathbf{n}$ is an $M \times 1$ vector containing the noise perturbing each of the receivers [34]. The channel matrix describes the structure of the antenna and wave propagation between the ports of the transmitter and the ports of the receiver. There are several ways to model a MIMO system depending on how we wish to describe the input and output signals. For example, we may consider the input signals to be the voltage sources in the antenna feeds or the wave forms sent through the transmission lines connected to the antenna ports. In this section of the paper we model the MIMO system using a scattering matrix, and consider the input and output signals in terms of spherical mode coefficients [17].

An antenna system's radiating and receiving properties can be described by the scattering matrix [17],

$$\begin{pmatrix} \mathbf{S}_{1,1} & \mathbf{S}_{1,2} \\ \mathbf{S}_{2,1} & \mathbf{S}_{2,2} \end{pmatrix} \begin{pmatrix} \boldsymbol{v} \\ \boldsymbol{\alpha} \end{pmatrix} = \begin{pmatrix} \boldsymbol{w} \\ \boldsymbol{\beta} \end{pmatrix}, \tag{2.2}$$

where $\boldsymbol{v}$ are the signals incoming to the ports of the antenna, $\boldsymbol{w}$ are the outgoing signals from the antenna, $\boldsymbol{\alpha}$ are the incoming spherical waves, $\boldsymbol{\beta}$ are the outgoing spherical waves, $\mathbf{S}_{1,1}$ is the reflection matrix with dimension $N \times N$, $\mathbf{S}_{2,2}$ is the matrix representing how the antenna couples incoming and outgoing spherical waves with dimension $\infty \times \infty$, $\mathbf{S}_{2,1}$ is the $\infty \times N$ matrix coupling the input signals to the antennas to the radiated spherical waves, and $\mathbf{S}_{1,2}$ is the $N \times \infty$ matrix coupling the incoming waves to the signals in the ports. The subscripts are used to denote that these matrices are parts of the scattering matrix. Here, we assume that our antenna is made of linear, passive, reciprocal materials, such as metals and dielectrics, making the antenna a reciprocal system. This means that the antenna behaves equivalently when receiving or transmitting [17].

There exists many different channel models to describe specific propagation environments [33, 34]. However, in this paper we aim to consider the most general scenario to provide a basis from which to construct general performance bounds for MIMO antennas. Many MIMO devices, *e.g.*, handsets or small electronics, can be considered to operate in uniform multipath environments. These environments are characterized by a large number of independent waves impinging on the antenna from all directions, see Fig. 2. These waves impinging on the sphere surrounding the antenna system are modeled by a Rayleigh channel in the spherical modes [10, 13, 23]. The Rayleigh channel $\mathbf{H}_{\mathrm{w}}$ is modeled by a random matrix with a complex Gaussian distribution that is uncorrelated and has zero mean [32, 34, 40]. Because the considered antenna is a reciprocal system it behaves equivalently when receiving or transceiving. Consequently, we model the transceiving channel as a Rayleigh channel as well.

The MIMO system in Fig. 1 is therefore simplified to a MIMO antenna in a spherical Rayleigh channel as in Fig. 2. This system is governed by the equation

$$\boldsymbol{w} = \mathbf{H}_{\mathrm{w}} \mathbf{S}_{1,1} \boldsymbol{v}, \tag{2.3}$$

when operating in transceiving mode. The instantaneous spectral efficiency of this system can be calculated by optimizing the time average over the modulation in the input signals, *i.e.*, $\mathbf{A} = \frac{1}{2}\mathcal{E}\left\{\boldsymbol{v}\boldsymbol{v}^{\mathrm{H}}\right\}$, where $\mathcal{E}\{\cdot\}$ denotes the temporal average. The matrix $\mathbf{A}$ is called the covariance matrix of the input signals. The optimization problem for instantaneous spectral efficiency is [34]

$$\begin{aligned} \underset{\mathbf{A} \succeq \mathbf{0}}{\text{maximize}} \quad & C = \log_2 \det(\mathbf{1} + \gamma \mathbf{H}_{\mathrm{w}} \mathbf{S}_{1,1} \mathbf{A} \mathbf{S}_{1,1}^{\mathrm{H}} \mathbf{H}_{\mathrm{w}}^{\mathrm{H}}) \\ \text{subject to} \quad & \mathrm{tr}(\mathbf{A}) = 1 \end{aligned} \tag{2.4}$$

where $\mathbf{1}$ is the identity matrix, input power is normalized to 1, and γ is the signal-to-noise ratio (SNR). In many applications the channel $\mathbf{H}_{\mathrm{w}}$ changes over time. It is then necessary to consider the ergodic spectral efficiency, *i.e.*, the spectral efficiency averaged over channel realizations, $\bar{C} = \mathcal{E}\{C\}$.

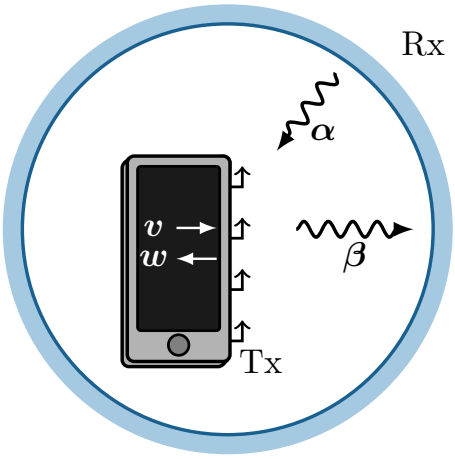

Figure 2: Schematic illustration of a MIMO antenna inside a spherical channel. The incoming and outgoing signals are depicted for the transceiving antenna as $\boldsymbol{v}$ and $\boldsymbol{w}$, and for the spherical channel as $\boldsymbol{\alpha}$ and $\boldsymbol{\beta}$, respectively.

To study the dependence of the system on the Rayleigh channel, consider a MIMO system with a finite and small number of ports N. Since the number of ports is small, the SNR can be considered to be large in each port, *i.e.*, $\gamma \mathbf{H}_{\mathrm{w}} \mathbf{S}_{1,1} \mathbf{A} \mathbf{S}_{1,1}^{\mathrm{H}} \mathbf{H}_{\mathrm{w}}^{\mathrm{H}} \succ \alpha \mathbf{1}$, $\alpha \gg 1$. The ergodic spectral efficiency can then be written as,

$$\begin{aligned} \bar{C} &= \mathcal{E}\left\{\log_2 \det(\gamma \mathbf{H}_{\mathrm{w}} \mathbf{S}_{1,1} \mathbf{A} \mathbf{S}_{1,1}^{\mathrm{H}} \mathbf{H}_{\mathrm{w}}^{\mathrm{H}})\right\} \\ &= \log_2 \det(\gamma) + \mathcal{E}\left\{\log_2 \det(\mathbf{H}_{\mathrm{w}})\right\} \\ &\quad + \mathcal{E}\left\{\log_2 \det(\mathbf{H}_{\mathrm{w}}^{\mathrm{H}})\right\} + \log_2 \det(\mathbf{S}_{1,1} \mathbf{A} \mathbf{S}_{1,1}^{\mathrm{H}}). \end{aligned} \tag{2.5}$$

The channel effect of such a system is therefore only an additive term in the spectral efficiency evaluation. Consider the correlation loss, defined as

$$\Delta \bar{C} = \bar{C} - \bar{C}_{\mathbf{1}}, \tag{2.6}$$

where $\bar{C}_{\mathbf{1}}$ is the equal power allocation solution. This quantity is independent of the additive channel contribution in (2.5). This implies that the physics of maximizing ergodic spectral efficiency is independent of the channel in uniform multipath environment, as long as the number of ports in the system is low [13]. Note that (2.6) only contains a temporal average over the input signals, significantly simplifying its evaluation.

Modelling the MIMO system using the scattering matrix is useful when studying channel phenomena. However, in this paper, we focus on how the design of the MIMO antenna impacts optimal spectral efficiency. Consider the region in Fig. 3a, we want to analyze how to construct the most effective MIMO antenna within this region. We must therefore switch our modelling from the abstract spherical mode amplitudes to quantities that let us incorporate antenna design as a variable.

The scattering matrix relation (2.2) can be rewritten in terms of port quantities

$$\mathbf{zi} = \mathbf{v}, \tag{2.7}$$

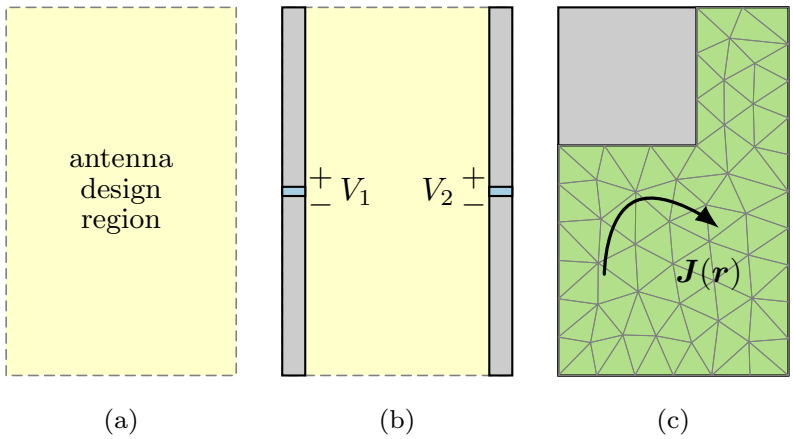

Figure 3: Possible full-wave models of a transmitter Tx from Fig. 2. (a) An antenna design region to be occupied by a MIMO system. (b) Two dipoles of fixed geometry are considered within the design region. The feeding voltages, confined to the blue regions, are controllable variables to be optimized for maximum capacity. (c) The current density, confined to the green region, is the controllable quantity. An optimized current is considered to be impressed in vacuum, the uncontrollable region is made from a given, yet arbitrary, material.

where $\mathbf{v}$ are the port voltages, $\mathbf{i}$ are the port currents, and $\mathbf{z}$ is the network impedance matrix [19, 35]. Here, we have moved our perspective to Fig. 3b. The network impedance matrix can either be calculated from the (measured) scattering matrix or from a full-wave EM model. This is useful when studying a fixed set of antennas, as is done in Sec. 3. We can further rewrite (2.7) in terms of meshed structures in order to use full-wave electromagnetic simulation techniques. In this paper we use method of moments (MoM) to simulate our systems, rewriting (2.7) as,

$$\mathbf{ZI} = \mathbf{V}, \tag{2.8}$$

where $\mathbf{I}$ is the current column matrix, $\mathbf{V}$ is the excitation column matrix, and $\mathbf{Z}$ is the impedance matrix [4], see Appendix A. This equation models the case in Fig. 3c, where the current can exist everywhere inside the design region. The current can be split into regions that are controlled or passively excited by the controlled region [14]. This formulation is very useful when optimizing the current to study all possible antenna structures in a region, which is done in Sec. 4.

3 Array Antenna Excitation

In this section we first consider a fixed antenna geometry, see Fig. 3b, in a Rayleigh channel and verify the conclusions of the previous section. Then, the excitation is optimized when the antenna is placed in an ideal channel and the maximum capacity given by a set of feeding ports is studied when the antenna's bandwidth for each port is prescribed and represented by the Q-factor. These fixed geometries are used to convey an intuition of how to induce optimal spectral efficiency.

The current on an antenna structure is modeled as a linear combination of currents excited by localized feeders, so-called port modes [20], see Fig. 3c,

$$\mathbf{I} = \mathbf{Z}^{-1}\mathbf{C}\mathbf{v} = \sum_p v_p \mathbf{I}_p, \tag{3.1}$$

where each port mode $\mathbf{I}_p$ corresponds to a unitary excitation of the p-th port, $\mathbf{Z}$ is the impedance matrix introduced in (2.8), and $\mathbf{C} \in \{0,1\}^{M\times P}$ is an indexation matrix defined element-wise as

$$C_{mp} = \begin{cases} 1 & p\text{-th port is placed at } m\text{-th position,} \\ 0 & \text{otherwise.} \end{cases} \tag{3.2}$$

A remarkable advantage of the port-mode representation is the reduction of the original $M \times M$ matrices, *i.e.*, of number of degrees of freedom, to $P \times P$, the number of ports. The construction of the impedance matrix (2.8) prior the reduction into port modes (3.1) is needed since it represents the full-wave electromagnetic behavior of the systems. The values of physical quantities defined in MoM-like (2.8) and port-like (2.7) representations are equivalent. To illustrate the transformation let $\mathbf{M} = \mathbf{M}^{\mathrm{H}} \in \mathbb{C}^{M\times M}$ represent a generic MoM operator, such as the reactance matrix $\mathbf{X}$. The following quadratic forms map this operator to its port equivalent, $\mathbf{m} \in \mathbb{C}^{P\times P}$,

$$m = \frac{1}{2}\mathbf{I}^{\mathrm{H}}\mathbf{M}\mathbf{I} = \frac{1}{2}\mathbf{v}^{\mathrm{H}}\mathbf{m}\mathbf{v}, \tag{3.3}$$

where

$$\mathbf{m} = \mathbf{C}^{\mathrm{H}}\mathbf{Z}^{-\mathrm{H}}\mathbf{M}\mathbf{Z}^{-1}\mathbf{C}. \tag{3.4}$$

Spectral efficiency is calculated through the covariance of the input signals. The quadratic forms that typically calculate antenna quantities can be rewritten in terms of the covariance of the port voltages. Conveniently, the port voltages is the only part of the antenna expressions that vary in time, therefore the temporal average can be confined to this variable. For example the input power can be written as,

$$\frac{1}{2}\mathcal{E}\left\{\mathbf{v}^{\mathrm{H}}\mathbf{r}_{\mathrm{r}}\mathbf{v}\right\} = \frac{1}{2}\operatorname{tr}\left(\mathcal{E}\left\{\mathbf{v}^{\mathrm{H}}\mathbf{r}_{\mathrm{r}}\mathbf{v}\right\}\right) = \frac{1}{2}\operatorname{tr}\left(\mathcal{E}\left\{\mathbf{r}_{\mathrm{r}}\mathbf{v}\mathbf{v}^{\mathrm{H}}\right\}\right) = \operatorname{tr}(\mathbf{r}_{\mathrm{r}}\mathbf{a}) = p, \tag{3.5}$$

where $\mathbf{a} = \mathcal{E}\left\{\mathbf{v}\mathbf{v}^{\mathrm{H}}\right\}/2$ is the covariance of the port voltages, p is the input power, and the cyclic properties of the trace have been utilized.

Applying the change of basis (3.3) and writing the problem in trace formulation, the spectral efficiency calculation (2.4) can be written in the port mode basis as

$$\begin{aligned} \underset{\mathbf{a}}{\text{maximize}} \quad & \log_2 \det\left(\mathbf{1} + \gamma \mathbf{s}\mathbf{a}\mathbf{s}^{\mathrm{H}}\right) \\ \text{subject to} \quad & \operatorname{tr}(\mathbf{r}_{\mathrm{r}}\mathbf{a}) = 1, \end{aligned} \tag{3.6}$$

where $\mathbf{r}_{\mathrm{t}} = \mathbf{s}^{\mathrm{H}}\mathbf{s}$ is the MoM radiation matrix, $\mathbf{s} = \mathbf{S}\mathbf{Z}^{-1}\mathbf{C}$ connects the antenna radiation with spherical modes in the farfield [9, 38]. Here, the total input power is normalized to unity, $p = 1\,\mathrm{W}$. This problem is only restricted by the input power to each port.

Antennas are most often optimized given certain restrictions to their performance quantities, the formulation of (3.6) enables us to add such restrictions as additional constraints. In this paper we investigate how bandwidth restrictions affect spectral efficiency optimization.

The Q-factor is an antenna quantity that estimates the fractional bandwidth [36, 44], see its definition in App. B. The connection between the Q-factor and the bandwidth is explicit for single input systems in free space but there exists no explicit quantity or expression for calculating the bandwidth for MIMO systems. However, each of the ports of a MIMO system is a single input system, if taken in isolation. Therefore, each of these ports have a well defined Q-factor based on their inputs. We can require a certain Q-factor of each of the ports in the system as a way of implicitly placing a requirement on the total systems bandwidth. However, the Q-factor is usually defined in relation to the system at resonance. For a multi-port system a single resonance of the total current is not always desired, thus the Q-factor of the system must be estimated in a different way. Here, we use the average of the magnetic and electric stored energies over the radiated power to estimate the bandwidth. This corresponds to adding the condition,

$$\frac{\mathcal{E}\left\{\mathbf{v}^{\mathrm{H}}\mathbf{w}_{\mathrm{x}}\mathbf{v}\right\}}{2p} = \mathrm{tr}(\mathbf{w}_{\mathrm{x}}\mathbf{a}) \leq Q, \tag{3.7}$$

where $\mathbf{w}_{\mathrm{x}}$ is the matrix giving the reactive power of the averaged stored energy, see App. B, Q is the required Q-factor, and the input power p is the same as the radiated power and normalized to 1 W.

The Q-factor constraint (3.7) is added to (3.6) to create the optimization problem that is investigated in this paper,

$$\begin{aligned} \underset{\mathbf{a}}{\text{maximize}} \quad & \log_2 \det\left(\mathbf{1} + \gamma \mathbf{s}\mathbf{a}\mathbf{s}^{\mathrm{H}}\right) \\ \text{subject to} \quad & \mathrm{tr}(\mathbf{r}_{\mathrm{r}}\mathbf{a}) = 1, \\ & \mathrm{tr}(\mathbf{w}_{\mathrm{x}}\mathbf{a}) \leq Q, \\ & \mathbf{a} \succeq 0. \end{aligned} \tag{3.8}$$

A problem on this form can be solved using commercially available software, such as matlab software for disciplined convex programming (CVX) [11], see [6]. However, it can be solved much more efficiently, and in such a way as to provide greater physical insight, using the method presented in [7]. The method is based on constructing a convex dual problem that can be solved semi-analytically. A brief outline of that procedure is covered here.

To formulate the dual of the optimization problem (3.8) we use that a problem with less conditions always bounds a problem with more conditions. We take an affine combination of the conditions restricting the original problem,

$$\begin{aligned} \min_{\nu} \max_{\mathbf{a}} \quad & \log_2 \det\left(\mathbf{1} + \gamma \mathbf{s}\mathbf{a}\mathbf{s}^{\mathrm{H}}\right) \\ \text{subject to} \quad & \mathrm{tr}\left[\left(\nu \mathbf{r}_{\mathrm{r}} + Q^{-1}\mathbf{x}_{\mathrm{w}}\right)\mathbf{a}\right] = (\nu + 1), \\ & \mathbf{a} \succeq 0, \end{aligned} \tag{3.9}$$

This problem is convex in the variable ν. The tightest bound on the solution of the original problem is found when the dual problem is minimized over ν [2]. The solution to this problem is found in [7] by incorporating the matrices of the first condition in (3.9) into the channel matrix of the system, see App. C. This recasts the system in a form where it can be solved by water filling [33, 34].

The water filling procedure is carried out by taking the singular value decomposition of the channel matrix. Each singular value represents the loss associated with feeding power in its corresponding mode. The optimal solution is found by iteratively allocating energy to the channels associated with the largest singular values [7, 33, 34]. The algorithm can be expressed as,

$$\begin{aligned} \text{maximize} \quad & \sum_{n=1}^{N} \log_2\left(1 + a_n \gamma \sigma_n^2\right) \\ \text{subject to} \quad & \sum_{n=1}^{N} a_n = 1, \end{aligned} \tag{3.10}$$

where $a_n \geq 0$ is the power allocation fraction in each channel, and σ_n is the singular value of the corresponding channel.

The singular values of the channel matrix are

$$\sigma_n^2 = \frac{1+\nu}{w_n/Q + \nu}, \tag{3.11}$$

where w_n are the eigenvalues of a set of modes, here referred to as energy modes [15]. The energy modes are calculated through the generalized eigenvalue problem, defined here over port mode matrices,

$$\mathbf{w}_{\mathrm{x}} \mathbf{v}_n = w_n \mathbf{r}_{\mathrm{r}} \mathbf{v}_n, \tag{3.12}$$

where $\mathbf{v}_n$ are the modal port voltages. These modes are similar to characteristic modes [21] in the sense that they have the property of orthogonal radiation patterns. In addition, they minimize the total energy stored by the antenna. This has the effect of implicitly maximizing the bandwidth of the modes with the lowest eigenvalues. Let us now consider a few examples to see how the solution to this optimization problem behaves.

3.1 Rayleigh Channel Dependence

The optimization problem (3.9) can be solved for a MIMO antenna in a complex propagation channel, by multiplying the matrix $\mathbf{s}$ with the channel matrix. However, the singular value decomposition (SVD) of the channel matrix (3.11) can no longer be found efficiently. For each ν considered in the optimization process, the SVD must be calculated numerically.

In Sec. 2 it was shown that the effect of a Rayleigh channel on the maximum spectral efficiency of a system with a low number of ports is additive. In Fig. 4, two centrally fed dipoles in a Rayleigh channel and an ideal channel have been optimized

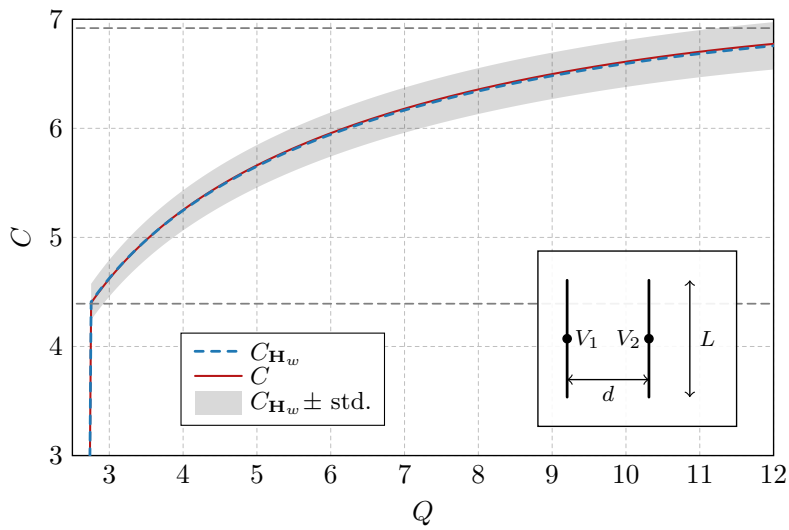

Figure 4: The maximal spectral efficiency of two centrally fed dipoles in a Rayleigh (the blue dashed line) and ideal channel (the solid red line). The gray area denotes the one standard deviation limit of the channel realizations. The dipoles have electrical size $L/\lambda = 0.49$, are separated $d/L = 0.3$, and the SNR is 20 dB. The dashed horizontal lines correspond to one and two ideal equal power allocation channels [7].

for maximum spectral efficiency. It can be seen that the antenna in an ideal channel follows the behaviour of the system in a Rayleigh channel. This shows that the ideal channel can be considered to understand the maximum spectral efficiency characteristics of an electrically small antenna design problem.

The horizontal dashed lines in Fig. 4 show the spectral efficiency of one and two ideal equal power allocation channels that do not take into account antenna geometry or channel effects. These lines serve as an indicator of how many pathways the system is utilizing [7]. The two dipoles can be seen to have solutions in between one and two ideal channels. Indicating that they are utilizing two channel pathways.

In Fig. 4, the spectral efficiency grows with Q. This can be misleading, and does not mean that higher capacity can be achieved by a narrow-band system. Spectral efficiency is a measure of the maximum bit rate that can be achieved on a 1 Hz bandwidth. By allowing a higher Q-factor in the optimization problem the solution can concentrate all spectral efficiency to a specific frequency. The true capacity can be calculated from the spectral efficiency by multiplying it by the bandwidth. An indication of the capacity can be found by considering the spectral efficiency divided by the required Q-factor, C/Q. This measure is adopted for the remaining results in the paper.

3.2 Example – Two Dipoles of Variable Separation Distance

The first example deals with two thin-strip dipoles of (resonant) length $L/\lambda = 0.49$ and width $L/W = 50$. The dipoles are made of perfect electric conductor (PEC) and separated by the distance d swept in the interval $d/L \in [0, 1]$.

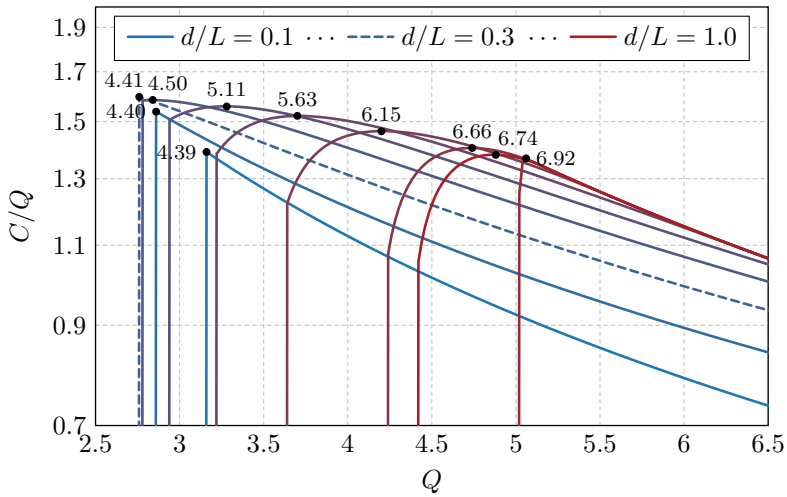

Figure 5: The maximal spectral efficiency with constrained Q for two thin-strip dipoles of separation distance d. Dot marks with numbers correspond to particular spectral efficiencies, evaluated at C/Q maximum. The SNR was set to 20 dB.

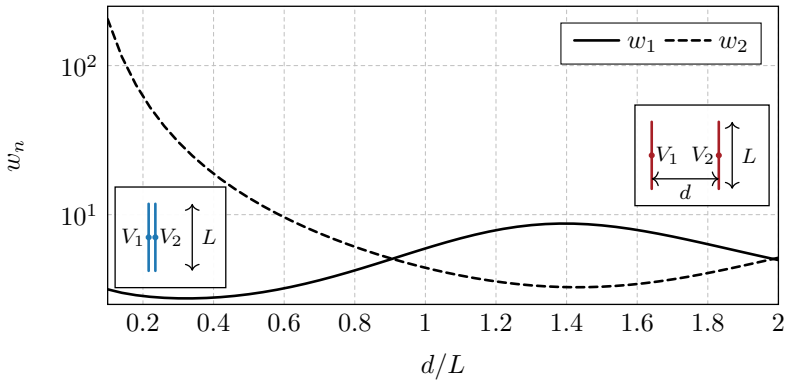

Figure 6: The eigenvalues of the energy port-modes w_n evaluated by (3.12) for an array of two in-parallel placed dipoles separated by the distance d.

The spectral efficiency C constrained by Q, expressed as C/Q, is shown in Fig. 5. It is seen that there exists an optimal distance, $d/L \approx 0.3$, for which C/Q is maximal. All the curves are bounded from the left by the fundamental bound on Q for two dipoles. For two dipoles separated by distance $d/L \approx 0.3$ that bound is $Q = 2.76$. This supports previous observations [22] that two mutually coupled dipoles might have lower Q than a single dipole (here $Q = 5.23$). The maximum spectral efficiency is found for the maximum separation distance, here $d/L = 1$. However, this curve does not dominate the others, even though it has the highest spectral efficiency. This is due to the high Q of the dipoles. When they are separated by a large distance they act as separate radiators and do not improve their joint Q-factor.

The sole input into the optimization procedure is the set of energy mode eigenvalues (3.12). Their dependence on the separation distance d/L is shown in Fig. 6. There are two types of modes, in-phase and out-of-phase modes, which become

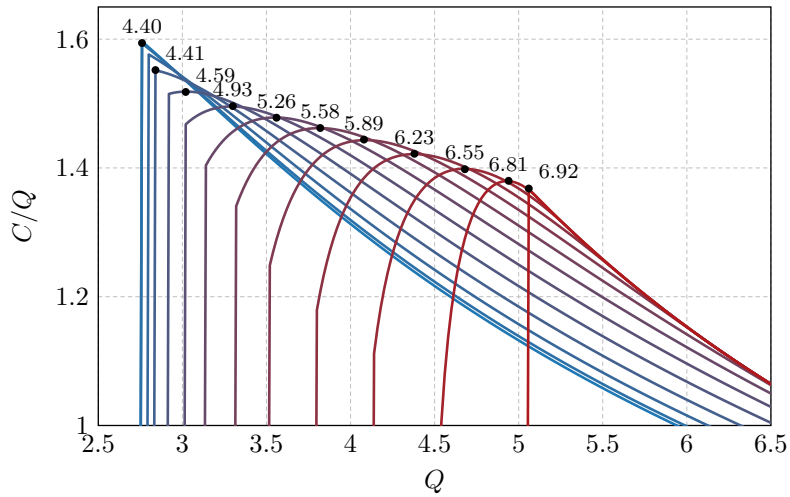

Figure 7: The maximal spectral efficiency with constrained Q for two thin-strip dipoles rotated by the angle φ. The dot marks with numbers correspond to particular spectral efficiencies, evaluated at C/Q maximum. The SNR is set to 20 dB.

degenerated at $d/L \approx 0.9$ and $d/L \approx 1.9$. The x-axis showing d/L parameter is extended to $d/L = 2$ in order to show at least two degeneracies.

3.3 Example – Two Dipoles Rotated by An Arbitrary Angle

Here, we study the dependence on the angle between the dipoles. The separation distance between two dipoles is fixed to the optimal value from the previous example, *i.e.*, $d/L = 0.3$. The dipoles are of the same dimensions, located at $x = -d/2$ and $x = d/2$, and the left dipole is parallel to z-axis. The axis of rotation for the right dipole coincides with the x-axis, see the insets of Fig. 7.

The results for optimization of C/Q are depicted in Fig. 7. Similar trends as in Fig. 5 are observed. The spectral efficiency over Q decreases rapidly with an increasing angle of rotation φ. Conversely, the spectral efficiency increases and reaches its maximum for $\varphi = \pi/2$, where the dipoles are crossed and able to utilize two times more spherical harmonics, *i.e.*, their radiation is relatively uncoupled. This is confirmed by the identical value of spectral efficiency, $C = 6.92$ for two distant dipoles in Fig. 5 and two dipoles rotated by angle $\varphi = \pi/2$ in Fig. 7. Similarly, as in the previous example, the cost for this performance in capacity is higher required bandwidth (Q). This conclusion is supported by Fig. 8, where the eigenvalues w_n are shown. They become degenerate for angle $\varphi = \pi/2$, *i.e.*, both states can be utilized equally.

3.4 Example – A Dipole Array of Various Number of Elements

The last example of this section studies the optimal capacity depending on the increasing number of dipoles in the linear array. Their separation distance is fixed

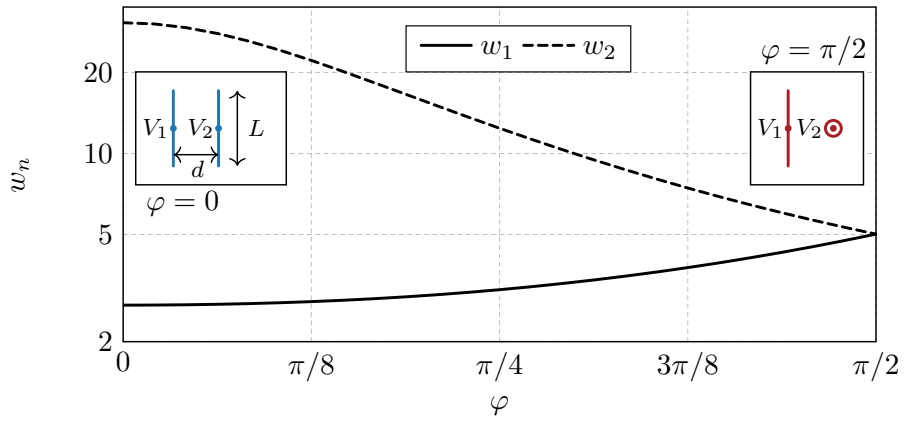

Figure 8: The eigenvalues of energy port-modes w_n evaluated by (3.12) for an array of two dipoles placed in-parallel and rotated by angle φ.

to $d/L = 0.3$, the dimensions of the individual radiators are the same as in the previous examples.

The course of the spectral efficiency constrained by Q is depicted in Fig. 9. It is obvious that the performance is significantly boosted with each dipole added to the array and, for a given number of radiators, the maximum of C/Q and the maximum of C coincide. The cost of the higher spectral efficiency is an increase of electrical size. For the sake of completeness, the eigenvalues w_n are depicted in Fig. 10. Adding more dipoles imply more available states for the optimization. The high-order eigenvalues grow rapidly, whereas the other ones are accumulated closer to the dominant eigenvalue, introducing additional degrees of freedom into the radiation process.

4 Bound on Antenna Design

In Sec. 3 the spectral efficiency is optimized through input parameters to ports for a fixed geometry. In order to formulate an upper bound on spectral efficiency that can be gained through antenna design we must make the antenna structure part of the optimization variable. In this section this is done through current optimization [15].

An antenna structure, *e.g.*, the structure depicted in Fig. 3b, radiates electromagnetic fields through the current that the excitation in the ports induces across it. In MoM this current is modelled through equivalent currents in free space. The equivalent current is represented through the basis functions that are connected to the mesh. Consider a MoM mesh covering the entire design region in Fig. 3a as in Fig. 3c, if this mesh is sufficiently dense it can support the equivalent current of any antenna structure that could be designed in the region. The technique of current optimization optimizes the weights of the basis functions of such a mesh. Because the equivalent current can represent the radiation properties of any antenna in the design region, an optimal current bounds those properties. However, antenna designs have several physical limitations to the current that they can induce, such

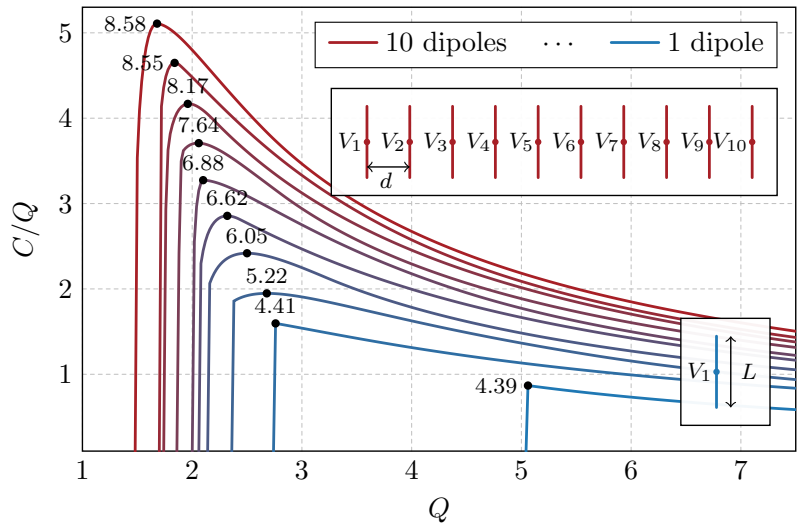

Figure 9: The optimized C/Q and the spectral efficiency C for the dipole array consisting of a variable number of thin-strip dipole elements (from one to ten). The dot marks with the numbers correspond to particular spectral efficiencies, evaluated at C/Q maximum. The SNR was set to 20 dB.

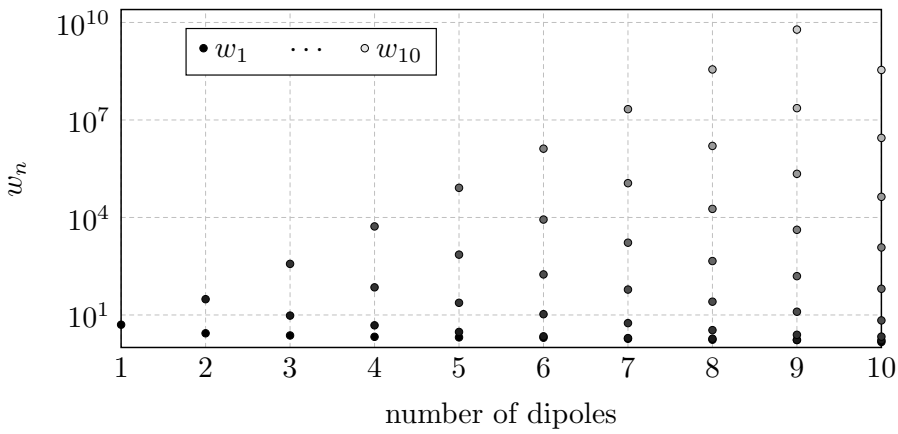

Figure 10: The eigenvalues of stored energy modes w_n for a dipole array consisting of a variable number of thin-strip dipole elements (from one to ten).

as feeding. The equivalent current does not share these restrictions and therefore can support current distributions that are not realizable but perform better than any antenna design. This ensures that the optimal value gained through current optimization is always equal to or greater than that gained through antenna design in the same region.

Optimizing spectral efficiency through current optimization has been treated extensively by the authors in [6, 7], and is only briefly reiterated here.

The optimization problem (3.8) can readily be rewritten in terms of the equivalent current. Take the covariance of the current, $\mathbf{P} = \mathcal{E}\left\{\mathbf{I}\mathbf{I}^{\mathrm{H}}\right\}/2$, as the optimization variable and replace all port mode matrices by their equivalent MoM matrices, see (3.3). The optimization problem is then written as

$$\begin{aligned} \text{maximize} \quad & \log_2 \det\left(\mathbf{1} + \gamma \mathbf{S}\mathbf{P}\mathbf{S}^{\mathrm{H}}\right) \\ \text{subject to} \quad & \operatorname{tr}(\mathbf{W}_{\mathrm{x}}\mathbf{P}) \leq Q \\ & \operatorname{tr}(\mathbf{R}_{\mathrm{r}}\mathbf{P}) = 1 \\ & \operatorname{rank}\mathbf{P} \leq N \\ & \mathbf{P} \succeq 0, \end{aligned} \tag{4.1}$$

where N is the number of degrees of freedom of the system. Here, the port positions are no longer fixed, only their number is specified. This problem can be solved in different ways depending on what we wish to investigate.

The optimization problem (4.1) can be made convex by dropping the rank constraint [7]. The problem can then be solved directly using freely available convex optimization software such as CVX [6, 11]. However, this method can become computationally cumbersome for bigger problems.

The problem can instead be solved using the method detailed in [7], see App. C. The solution is equivalent to replacing the singular values in (3.10), with those calculated through (3.11) using the energy mode eigenvalues W_n calculated by the generalized eigenvalue problem,

$$\mathbf{X}_{\mathrm{w}}\mathbf{I}_n = W_n \mathbf{R}_{\mathrm{r}}\mathbf{I}_n. \tag{4.2}$$

These modes have the same properties as their port equivalents (3.12), *i.e.*, orthogonal radiation patterns and minimization of the total stored energy.

4.1 Rayleigh Channel Dependence

When optimizing over the current density the number of channels in (2.4) can no longer be considered small. Therefore, we must analyze the impact of the Rayleigh channel on the optimization results. Consider (4.1) with the objective function,

$$C = \log_2 \det\left(\mathbf{1} + \gamma \mathbf{H}_{\mathrm{w}}\mathbf{S}\mathbf{P}\mathbf{S}^{\mathrm{H}}\mathbf{H}_{\mathrm{w}}^{\mathrm{H}}\right). \tag{4.3}$$

This is done, as in Sec. 3.1, by numerically calculating the SVD of the channel matrix for each ν.

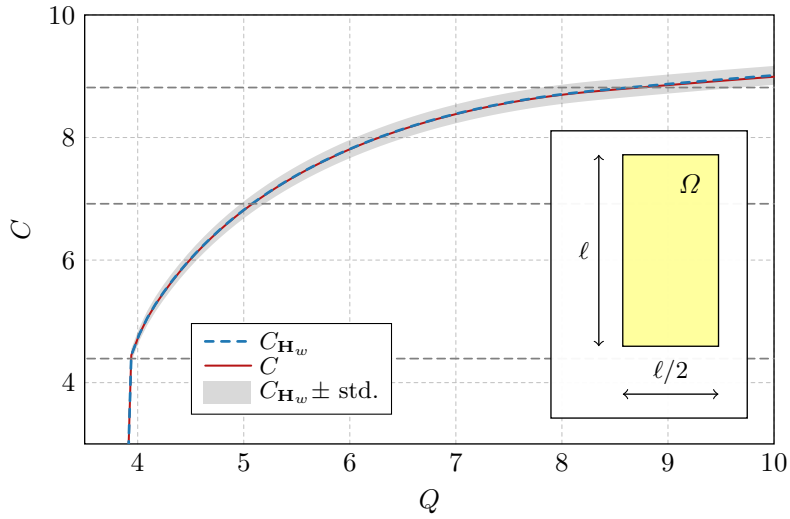

Figure 11: Maximum spectral efficiency of a $ka = 1$, $\ell \times \ell/2$ plate in a Rayleigh (the blue dashed line), and an ideal channel (the solid red line). The gray area denotes one standard deviation from the average of the Rayleigh channel case. The dashed horizontal lines correspond to one, two, and three ideal equal power allocation channels [7].

In Fig. 11 the current on a $ka = 1$ plate has been optimized for maximal spectral efficiency with and without the inclusion of an uniform Rayleigh channel. The average of the Rayleigh channel realizations has the same performance as the plate in an ideal spherical channel. This supports the claims in [6, 7] that the channel can be neglected when studying the fundamentals of antenna design for optimal spectral efficiency.

The standard deviation of the Rayleigh channel realizations for the plate in Fig. 11 is significantly smaller than what can be seen for two dipoles in Fig. 4. This is due to the added degrees of freedom in optimizing an entire plate. The plate can support higher order modes at lower Q-values and its current can be tailored to specific channel realizations.

4.2 Sub-region Antennas

Antennas inside communication devices are, in general, much smaller than the total device size [43]. This means that only a sub-region of the device is dedicated to antenna design. The antennas therein excite currents across the entire device that contribute to communication. From an optimization perspective this can be seen as only controlling the current within the antenna sub-region. The optimization of arrays through their port quantities in Sec. 3 is similar to this concept. The ports control the current on the dipole on a very small sub-region of the antenna. In this section this concept is generalized to controlling the current in larger sub-regions, see Fig. 3c. Optimizing the current on a sub-region for maximal spectral efficiency calculates a bound on the spectral efficiency available from designing an antenna in

a sub-region of a device.

It is possible to find the optimal solution to (4.1) when controlling only a sub-region of the device by reformulating the problem in the controlled currents of the sub-region [7]. This is interesting to investigate since bandwidth and Q-factor are usually harshly restricted by reducing the antenna size [3, 41].

4.3 Modal Analysis

Rather than solving the entire optimization problem (4.1) it is possible to evaluate a design geometry much more efficiently by studying its energy modes. The solution of (4.1) is only dependent on the singular values of the channel (3.11), see App. C. When calculating the singular values, the only part connected to the geometry of the antenna are the eigenvalues of the energy modes W_n. By studying the magnitude of these eigenvalues it is possible to evaluate how well a geometry performs in terms of maximal spectral efficiency [7]. This serves as a fast method to compare different design strategies to each other without solving the full optimization problem. All that is required is to solve the generalized eigenvalue problem (4.2).

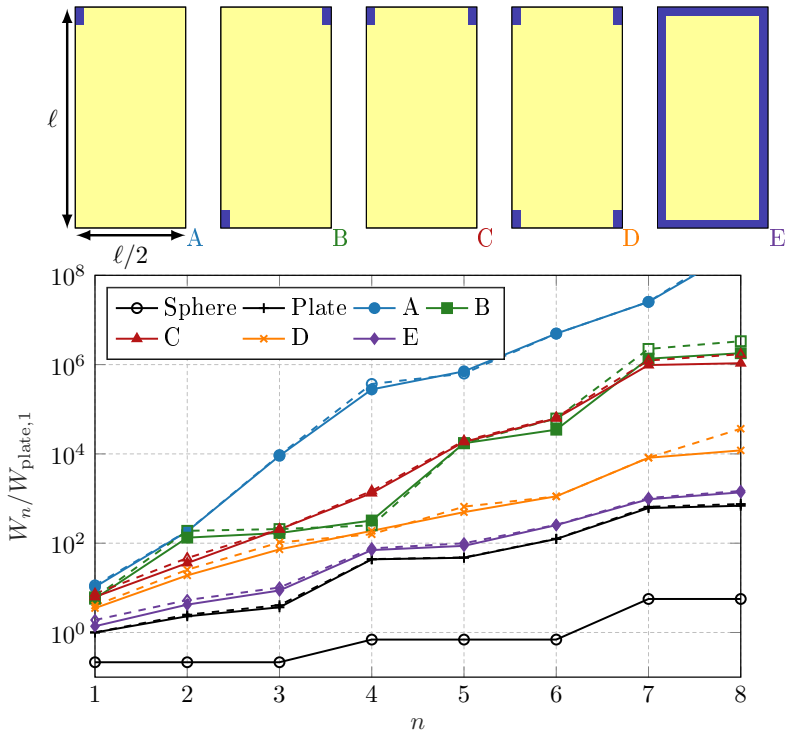

Figure 12: The eigenvalues w_n of a spherical shell, a rectangular plate with aspect ratio 2 : 1, and several of its sub-region arrangements with size $0.1\ell \times 0.05\ell$ for case A-D and width 0.05ℓ for case E, where the current is controlled inside the blue regions. All the eigenvalues have been normalized to the first energy mode of the full plate, the electrical size is $ka = 1$, where k is the wave number, and a is the radius of the smallest sphere circumscribing the entire structure. The dashed lines correspond to the characteristic mode currents evaluated in the Rayleigh quotient (4.4) [1].

Consider the placement of sub-regions for antenna design within a device. Which orientation of sub-region has the greatest potential spectral efficiency can be evaluated by comparing their energy mode eigenvalues. In Fig. 12, five different sub-region eigenvalues, as well as the plate and circumscribing spherical shell eigenvalues, are shown normalized to the first eigenvalue of controlling the current over the entire plate. By studying how close each of the sub-region cases come to the eigenvalues of the full plate we can evaluate how well they induce the full performance of the plate. In Fig. 12, we see that there is a considerable gap between the eigenvalue of the full plate compared to small segregated sub-regions. This contrasts to the results in [7] where it was shown that, when restricting (4.1) by efficiency, it is possible to induce the entire structures available performance while only feeding a couple of small sub-regions. However, in case E the current is controlled in a loop around the plate, here the eigenvalues are almost the same as that of the full plate. We can also see that the two diagonally placed elements in case B outperform the two elements in case C for all mode indices except the second one. This is similar to the case in [7] due to the first and second order modes being induced diagonally across the plate. Therefore, the two diagonally situated sub-regions do not effectively induce the second mode across the opposite diagonal. The eigenvalues of the circumscribing spherical shell have been included as a reference, and we can see that they are significantly lower than those of the plate.

The dashed lines in Fig. 12 correspond to the characteristic mode currents evaluated in the Rayleigh quotient of the eigenvalue problem (4.2), *i.e.*,

$$W_{\mathrm{c},n} = \frac{\mathbf{I}_{\mathrm{c},n}^{\mathrm{H}} \mathbf{X}_{\mathrm{w}} \mathbf{I}_{\mathrm{c},n}}{\mathbf{I}_{\mathrm{c},n}^{\mathrm{H}} \mathbf{R}_{\mathrm{r}} \mathbf{I}_{\mathrm{c},n}}, \tag{4.4}$$

where $\mathbf{I}_{\mathrm{c},n}$ are the characteristic mode currents [21]. These values indicate how well the characteristic mode currents perform in the metric of energy modes. In Fig. 12, we see that the characteristic modes basically overlap the energy mode eigenvalues for all considered cases. This indicates that the characteristic modes are a good tool for MIMO antenna design, validating previous design methodologies [27, 28, 29].

4.4 Sub-region Optimization

The full problem (4.1) can be solved efficiently for the ideal channel case. In Fig. 13, the spectral efficiency over Q is depicted for the electrical size $ka = 1$ as a function of the required Q-factor. This Pareto-type curve delimits the feasible region of the problem and reveals that the capacity and the Q-factor are strictly conflicting parameters. Here, it is evident that there is a preferred Q-factor for optimal spectral efficiency for different sizes and geometries found at the maximum of the curves.

The dashed gray lines in Fig. 13 depict the equal power allocation channels. When the solution of the different sub-region cases passes one of these lines it is utilizing at least that many different channels to induce optimal spectral efficiency. This number is the structures number of effective modes for a certain allowed Q-factor. The number of effective modes can be estimated from Fig. 12 by multiplying the eigenvalues by their normalization, in this case $W_{\mathrm{plate},1} = 3.92$, and counting the

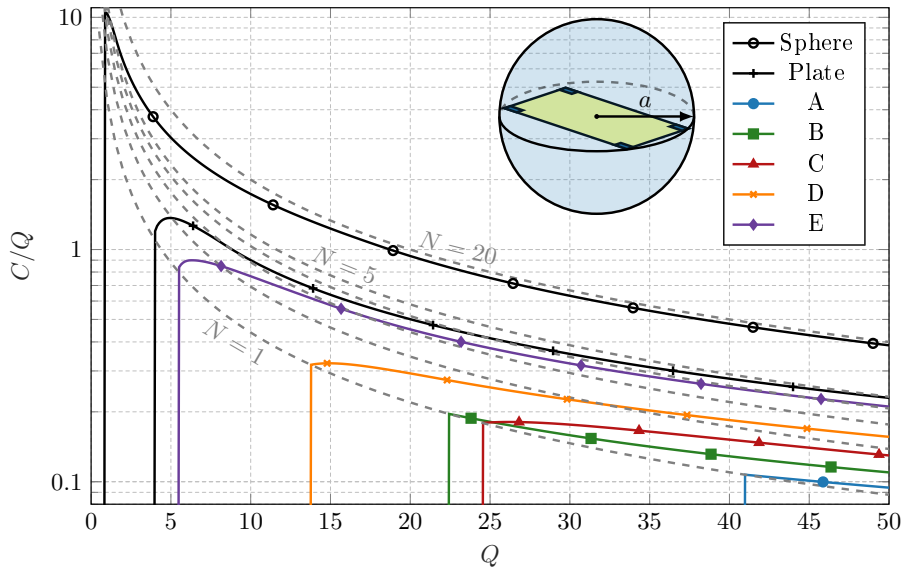

Figure 13: The optimal spectral efficiency over Q for the $ka = 1$ spherical shell, plate with aspect ratio $2:1$, and its sub-regions presented in Fig. 12, for different Q-factor restrictions. The dashed gray lines correspond to increasing numbers of ideal equal power allocation channels. The SNR has been set to $\gamma = 20$.

number of eigenvalues below $W_n = Q$. This is the limit for what is considered an effective mode, which can be found by studying when the asymptotics of (3.11) are stable for all ν [7]. When the number of ports is restricted by a certain number, in (4.1), the spectral efficiency over Q maximally reaches the dashed gray curve associated with that number of ideal channels.

It is evident that the small segregated sub-regions from case A to D do not effectively induce the available spectral efficiency of the full plate, the loop region is more efficient utilizing higher order modes. In contrast to the case studied in [7], that was restricted by efficiency, this gap between the sub-regions and the full plate remains the same when the size of the plate is reduced. Instead of narrowing the gap between the full plate and its sub-regions, as in [7], a reduction of size makes the sub-region solution unfeasible, due to the lower Q-factor bound [5]. Therefore, we can conclude that the optimal performance of the embedded MIMO antennas is more restricted by the limited bandwidth than the requirements on radiation efficiency.

4.5 Raised Sub-Regions

For many applications where embedded antennas are used, such as mobile phones, the antennas are not truly embedded inside the ground plane. Normally there is a substrate layer, or edge, that the antennas have been designed upon [43]. In the top of Fig. 14, case D from Fig. 12 with its regions raised above the ground plane as well as a rim region, is illustrated. Here the gap between the regions and the ground plane is not filled with any material. The performance of these controlled

regions is shown in Fig. 14 in terms of spectral efficiency over Q. The edge region performs comparably to that of case E in Fig. 13, only giving slightly worse results. The performance of case D has been considered when the placement of the regions is shifted in from the edge. The cost of moving away from the edge can be seen in Fig. 14. By shifting incrementally we can see that we quickly loose a significant amount of performance. This effect may be due to the fact that currents need to flow around the outer edges of the regions rather than being fed directly along the plate. In this case the regions are only connected to the ground plane on two edges, if all edges are connected the loss is even greater. Such a case is similar to when the regions are fully embedded within the ground plane. Comparing the un-shifted regions in Fig. 14 to Fig. 13, it is clear that the performance does not increase dramatically when raising the regions above the ground plane.

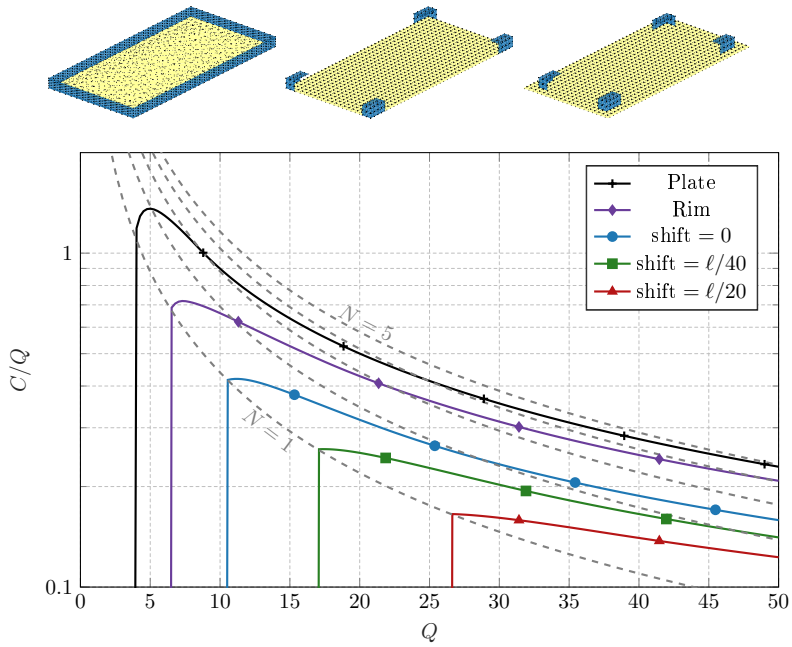

Figure 14: The optimal spectral efficiency over Q for the $ka = 1$ plate with aspect ratio $2:1$, the plate fed by a $\ell/20$ high rim region, and case D, present in Fig. 12 with its regions raised $\ell/20$ above the ground plane, as well as when those regions are shifted in a number of mesh cells towards the center as shown above. The restricting Q-factor has been swept and the SNR has been set to $\gamma = 20$.

5 Conclusions

The optimal spectral efficiency bound of a MIMO antenna in a Rayleigh and an ideal channel has been considered when restricted by the Q-factor. It was shown that the Rayleigh channel does not affect the characteristics of the optimal spectral efficiency bound. The Pareto-type bound has been illustrated in spectral efficiency over Q, where a certain Q-factor was shown to be Pareto optimal.

It has been shown that a set of modes known as energy modes, as well as characteristic modes, serves as a useful design tool when analyzing performance of MIMO antennas. The conclusion that a set of properly weighted characteristic modes approximately form an optimal current for capacity can be utilized in practice, specifically since simultaneous excitation of characteristic modes is well explored. However, due to the harsh penalties on stored energy when reducing the design region, it has been concluded that it is not possible to reach the full potential of the plate while only feeding it with a set of small segregated sub-regions. However, the use of a connected loop region was shown to be much more efficient. The placement of these regions has also been analyzed, and it could be seen that the performance quickly deteriorated when they were moved away from the edge of the structure.

The modal analysis illustrated in this paper could also be carried out on designed antennas to evaluate their adherence to the principals suggested here. Generalizing this method to include several different design parameters remains an interesting future prospect.

A Electric Field Integral Equation

All antenna structures in this paper are modeled as perfectly conducting bodies with the electric field integral equation (EFIE), [4], which relates tangential component of incident and scattered electric fields as

$$\hat{\boldsymbol{n}} \times \boldsymbol{E}_{\mathrm{i}}(\boldsymbol{r}) = -\hat{\boldsymbol{n}} \times \boldsymbol{E}_{\mathrm{s}}(\boldsymbol{r}), \tag{A.1}$$

where $\boldsymbol{E}_{\mathrm{i}}$ is the incident field, $\boldsymbol{E}_{\mathrm{s}}$ is the scattered field

$$\boldsymbol{E}_{\mathrm{s}}(\boldsymbol{r}) = -\mathrm{j}kZ_0 \int_{\Omega} \mathbf{G}(\boldsymbol{r}, \boldsymbol{r}') \cdot \boldsymbol{J}(\boldsymbol{r}') \, \mathrm{d}S', \tag{A.2}$$

Z_0 is the impedance of vacuum, k is wavenumber, and $\mathbf{G}$ denotes the free-space dyadic Green's function defined as

$$\mathbf{G}(\boldsymbol{r}, \boldsymbol{r}') = \left(\mathbf{1} + \frac{\nabla\nabla}{k^2}\right) \frac{\mathrm{e}^{-\mathrm{j}k|\mathbf{r}-\mathbf{r}'|}}{4\pi\,|\mathbf{r}-\mathbf{r}'|} \tag{A.3}$$

with $\mathbf{1}$ being the identity dyadic.

By applying a suitable set of basis functions

$$\boldsymbol{J}(\boldsymbol{r}) \approx \sum_n I_n \boldsymbol{\psi}_n(\boldsymbol{r}) \tag{A.4}$$

and the same set as testing functions (Galerkin method), the relation (A.1) transforms into algebraic form

$$\mathbf{ZI} = \mathbf{V}, \tag{A.5}$$

where the impedance matrix $\mathbf{Z} = [Z_{nm}] \in \mathbb{C}^{N\times N}$ and excitation vector $\mathbf{V} = [V_n] \in \mathbb{C}^{N\times 1}$ are defined element-wise as

$$Z_{nm} = -\mathrm{j}kZ_0 \int_{\Omega}\int_{\Omega} \boldsymbol{\psi}_n(\boldsymbol{r}) \cdot \mathbf{G}(\boldsymbol{r}, \boldsymbol{r}') \cdot \boldsymbol{\psi}_m(\boldsymbol{r}') \, \mathrm{d}S \, \mathrm{d}S', \tag{A.6}$$

and

$$V_n = \int_{\Omega} \boldsymbol{\psi}_n(\boldsymbol{r}) \cdot \boldsymbol{E}_{\mathrm{i}}(\boldsymbol{r}) \, \mathrm{d}S, \tag{A.7}$$

respectively.

B Definition of Q-factor

The Q-factor is defined as

$$Q = \frac{2\omega \max\{W_{\mathrm{m}}, W_{\mathrm{e}}\}}{P_{\mathrm{r}}}, \tag{B.1}$$

where the stored magnetic and electric energies are

$$\omega W_{\mathrm{m}} = \frac{1}{8}\mathbf{I}^{\mathrm{H}}\left(\omega\frac{\partial \mathbf{X}}{\partial \omega} + \mathbf{X}\right)\mathbf{I}, \tag{B.2a}$$

$$\omega W_{\mathrm{e}} = \frac{1}{8}\mathbf{I}^{\mathrm{H}}\left(\omega\frac{\partial \mathbf{X}}{\partial \omega} - \mathbf{X}\right)\mathbf{I}, \tag{B.2b}$$

the radiated power is defined as

$$P_{\mathrm{r}} = \frac{1}{2}\mathbf{I}^{\mathrm{H}}\mathbf{R}\mathbf{I}. \tag{B.3}$$

and $\mathbf{Z} = \mathbf{R} + \mathrm{j}\mathbf{X}$ is impedance matrix, see Appendix A. For purposes of this paper, the stored energy matrix is introduced as

$$\mathbf{W}_{\mathrm{x}} = \frac{1}{2}\omega\frac{\partial \mathbf{X}}{\partial \omega}. \tag{B.4}$$

C SVD of channel matrix

The optimal solution of (3.9) is found by writing the system on the form (3.10). This is achieved through a change of variables. Define the matrix

$$\mathbf{r}_{\nu} = \frac{1}{(\nu+1)}\left(\nu\mathbf{r}_{\mathrm{r}} + Q^{-1}\mathbf{w}_{\mathrm{x}}\right). \tag{C.1}$$

This matrix is positive semi-definite for sufficiently large antenna sizes, and appropriate values of ν. Positive semi-definite matrices can be decomposed with the Cholesky decomposition, $\mathbf{r}_{\nu} = \mathbf{b}^{\mathrm{H}}\mathbf{b}$. With this decomposition the condition in (3.10) can be rewritten as,

$$\mathcal{E}\left\{\mathbf{v}^{\mathrm{H}}\mathbf{r}_{\nu}\mathbf{v}\right\} = \mathrm{tr}(\mathbf{r}_{\nu}\mathbf{a}) = \mathrm{tr}(\mathbf{b}\mathbf{a}\mathbf{b}^{\mathrm{H}}) = \mathrm{tr}(\widetilde{\mathbf{a}}), \tag{C.2}$$

where the cyclic permutation of the trace has been utilized and $\widetilde{\mathbf{a}} = \mathbf{b}\mathbf{a}\mathbf{b}^{\mathrm{H}}$ is a change of variables. With this change of variables (3.9) is written as

$$\begin{aligned} \min_{\nu} \max_{\widetilde{\mathbf{a}}} \quad & \log_2 \det(\mathbf{1} + \gamma\mathbf{s}\mathbf{b}^{-1}\widetilde{\mathbf{a}}\mathbf{b}^{-\mathrm{H}}\mathbf{s}^{\mathrm{H}}) \\ \text{subject to} \quad & \mathrm{tr}(\widetilde{\mathbf{a}}) = 1. \end{aligned} \tag{C.3}$$

This is a problem that can be solved by water filling [33, 34], as in (3.10), with the channel matrix, $\mathbf{h} = \mathbf{s}\mathbf{b}^{-1}$. All that is required is the singular value decomposition of $\mathbf{h}$. The singular values can be calculated from the eigenvalues of the matrix times itself,

$$\operatorname{svd}(\mathbf{h}) = (\operatorname{eig}(\mathbf{h}\mathbf{h}^{\mathrm{H}}))^{1/2} = (\operatorname{eig}(\mathbf{s}\mathbf{r}_{\nu}^{-1}\mathbf{s}^{\mathrm{H}}))^{1/2}. \tag{C.4}$$

The eigenvalues can be determined by utilizing the decomposition of the radiation matrix, $\mathbf{r}_{\mathrm{r}} = \mathbf{s}^{\mathrm{H}}\mathbf{s}$. Putting this into (C.4),

$$\begin{aligned}\operatorname{eig}(\mathbf{s}\mathbf{r}_{\nu}^{-1}\mathbf{s}^{\mathrm{H}}) &= \operatorname{eig}((\nu+1)\left(\nu + Q^{-1}\mathbf{s}^{-\mathrm{H}}\mathbf{x}_{\mathrm{w}}\mathbf{s}^{-1}\right)^{-1}) \\ &= (\nu+1)\left(\nu + Q^{-1}\operatorname{eig}(\mathbf{s}^{-\mathrm{H}}\mathbf{x}_{\mathrm{w}}\mathbf{s}^{-1})\right)^{-1}.\end{aligned} \tag{C.5}$$

The eigenvalues $\operatorname{eig}(\mathbf{s}^{-\mathrm{H}}\mathbf{x}_{\mathrm{w}}\mathbf{s}^{-1})$ are determined from the generalized eigenvalue problem (3.12),

$$\mathbf{x}_{\mathrm{w}}\mathbf{v}_n = w_n\mathbf{r}_{\mathrm{r}}\mathbf{v}_n. \tag{C.6}$$

This gives the singular values (3.11),

$$\sigma_n^2 = \frac{(1+\nu)}{w_n/Q + \nu}. \tag{C.7}$$

Acknowledgment

This work was supported by the Swedish foundation for strategic research (SSF) under the program applied mathematics and the project Complex analysis and convex optimization for electromagnetic design.

References

[1] H. Alroughani, J. Ethier, and D. A. McNamara. "Orthogonality properties of sub-structure characteristic modes". *Microwave Opt. Techn. Lett.* 58 (2) (2016): pp. 481–486.

[2] S. P. Boyd and L. Vandenberghe. "Convex Optimization". Cambridge Univ. Pr., 2004.

[3] M. Capek, M. Gustafsson, and K. Schab. "Minimization of antenna quality factor". *IEEE Trans. Antennas Propag.* 65 (8) (2017): pp. 4115–4123.

[4] W. C. Chew, M. S. Tong, and B. Hu. "Integral Equation Methods for Electromagnetic and Elastic Waves". Vol. 12. Morgan & Claypool, 2008.

[5] M. Cismasu and M. Gustafsson. "Antenna bandwidth optimization with single frequency simulation". *IEEE Trans. Antennas Propag.* 62 (3) (2014): pp. 1304–1311.

[6] C. Ehrenborg and M. Gustafsson. "Fundamental bounds on MIMO antennas". *IEEE Antennas Wirel. Propag. Lett.* 17 (1) (2018): pp. 21–24.

[7] C. Ehrenborg and M. Gustafsson. "Physical bounds and radiation modes for MIMO antennas". *IEEE Trans. Antennas Propag.* (2020).

[8] M. Franceschetti, M. D. Migliore, and P. Minero. "The capacity of wireless networks: information-theoretic and physical limits". *IEEE Trans. Inf. Theory* 55 (8) (2009): pp. 3413–3424.

[9] A. A. Glazunov, M. Gustafsson, and A. Molisch. "On the physical limitations of the interaction of a spherical aperture and a random field". *IEEE Trans. Antennas Propag.* 59 (1) (2011): pp. 119–128.

[10] A. A. Glazunov, M. Gustafsson, A. Molisch, F. Tufvesson, and G. Kristensson. "Spherical vector wave expansion of gaussian electromagnetic fields for antenna-channel interaction analysis". *IEEE Trans. Antennas Propag.* 3 (2) (2009): pp. 214–227.

[11] M. Grant and S. Boyd. *CVX: Matlab Software for Disciplined Convex Programming, version 2.1*. `http://cvxr.com/cvx`. 2018.

[12] M. Gustafsson, M. Capek, and K. Schab. "Tradeoff between antenna efficiency and Q-factor". *IEEE Trans. Antennas Propag.* 67 (4) (2019): pp. 2482–2493.

[13] M. Gustafsson and S. Nordebo. "On the spectral efficiency of a sphere". *Prog. Electromagn. Res.* 67 (2007): pp. 275–296.

[14] M. Gustafsson and S. Nordebo. "Optimal antenna currents for Q, superdirectivity, and radiation patterns using convex optimization". *IEEE Trans. Antennas Propag.* 61 (3) (2013): pp. 1109–1118.

[15] M. Gustafsson, D. Tayli, C. Ehrenborg, M. Cismasu, and S. Nordebo. "Antenna current optimization using MATLAB and CVX". *FERMAT* 15 (5) (2016): pp. 1–29.

[16] M. Gustafsson, D. Tayli, and M. Cismasu. "Physical bounds of antennas". In: *Handbook of Antenna Technologies*. Ed. by Z. N. Chen. Springer-Verlag, 2015, pp. 197–233.

[17] J. E. Hansen, ed. "Spherical Near-Field Antenna Measurements". IEE electromagnetic waves series 26. Peter Peregrinus Ltd., 1988.

[18] R. C. Hansen. "Electrically Small, Superdirective, and Superconductive Antennas". John Wiley & Sons, 2006.

[19] R. F. Harrington. "Field Computation by Moment Methods". Macmillan, 1968.

[20] R. F. Harrington and J. R. Mautz. "Control of radar scattering by reactive loading". *IEEE Trans. Antennas Propag.* 20 (4) (1972): pp. 446–454.

[21] R. F. Harrington and J. R. Mautz. "Theory of characteristic modes for conducting bodies". *IEEE Trans. Antennas Propag.* 19 (5) (1971): pp. 622–628.

[22] P. Hazdra, M. Capek, and J. Eichler. "Radiation Q-factors of thin-wire dipole arrangements". *IEEE Antennas Wirel. Propag. Lett.* 10 (2011): pp. 556–560.

[23] W. C. Jakes and D. Cox. "Microwave Mobile Communications". IEEE Press, 1994.

[24] L Jelinek and M Capek. "Optimal currents on arbitrarily shaped surfaces". *IEEE Trans. Antennas Propag.* 65 (1) (2017): pp. 329–341.

[25] L. Jelinek, K. Schab, and M. Capek. "The radiation efficiency cost of resonance tuning". *IEEE Trans. Antennas Propag.* 66 (12) (2018): pp. 6716–6723.

[26] L. Kundu. "Information-Theoretic Limits on MIMO Antennas". PhD thesis. North Carolina State University, 2016.

[27] H. Li, Z. Miers, and B. K. Lau. "Design of orthogonal MIMO handset antennas based on characteristic mode manipulation at frequency bands below 1 GHz". *IEEE Trans. Antennas Propag.* 62 (5) (2014): pp. 2756–2766.

[28] D. Manteuffel and R. Martens. "A concept for MIMO antennas on small terminals based on characteristic modes". In: *International Workshop on Antenna Technology (iWAT).* 2011.

[29] Z. Miers, H. Li, and B. K. Lau. "Design of bandwidth-enhanced and multiband MIMO antennas using characteristic modes". *IEEE Antennas Wirel. Propag. Lett.* 12 (2013): pp. 1696–1699.

[30] M. D. Migliore. "Horse (electromagnetics) is more important than horseman (information) for wireless transmission". *IEEE Trans. Antennas Propag.* 67 (4) (2019): pp. 2046–2055.

[31] M. Migliore. "On electromagnetics and information theory". *IEEE Trans. Antennas Propag.* 56 (10) (2008): pp. 3188–3200.

[32] K. S. Miller. "Complex Stochastic Processes". Addison–Wesley Publishing Company, Inc., 1974.

[33] A. F. Molisch. "Wireless Communications". second. John Wiley & Sons, 2011.

[34] A. Paulraj, R. Nabar, and D. Gore. "Introduction to Space-Time Wireless Communications". Cambridge University Press, 2003.

[35] D. M. Pozar. "Microwave Engineering". third. John Wiley & Sons, 2005.

[36] K. Schab, L. Jelinek, M. Capek, C. Ehrenborg, D. Tayli, G. A. Vandenbosch, and M. Gustafsson. "Energy stored by radiating systems". *IEEE Access* 6 (2018): pp. 10553 –10568.

[37] P. S. Taluja and B. L. Hughes. "Fundamental capacity limits on compact MIMO-OFDM systems". In: *IEEE International Conference on Communications (ICC).* 2012, pp. 2547–2552.

[38] D. Tayli, M. Capek, L. Akrou, V. Losenicky, L. Jelinek, and M. Gustafsson. "Accurate and efficient evaluation of characteristic modes". *IEEE Trans. Antennas Propag.* (2018): pp. 1–10.

[39] G. A. E. Vandenbosch. "Reactive energies, impedance, and Q factor of radiating structures". *IEEE Trans. Antennas Propag.* 58 (4) (2010): pp. 1112–1127.

[40] R. Vaughan and J. Bach Andersen. "Channels, Propagation and Antennas for Mobile Communications". Institution of Electrical Engineers, 2003.

[41] J. Volakis, C. C. Chen, and K. Fujimoto. "Small Antennas: Miniaturization Techniques & Applications". McGraw-Hill, 2010.

[42] H. A. Wheeler. "Small antennas". *IEEE Trans. Antennas Propag.* 23 (4) (1975): pp. 462–469.

[43] K.-L. Wong. "Planar Antennas for Wireless Communications". John Wiley & Sons, 2003.

[44] A. D. Yaghjian and S. R. Best. "Impedance, bandwidth, and Q of antennas". *IEEE Trans. Antennas Propag.* 53 (4) (2005): pp. 1298–1324.